

A simple model of the hurricane boundary layer

By Roger K. Smith *

Meteorological Institute, University of Munich, Germany

August 5, 2002

Abstract

A simple, steady, moist, axisymmetric, constant depth, slab model for the hurricane boundary layer is investigated. High-resolution solutions of the boundary layer equations are obtained by integrating inwards from some large radius, at which it is assumed that geostrophic balance and convective-radiative balance exists. In all the solutions obtained, the tangential wind speed in the boundary layer approaches that above the boundary layer in the inner core region and the maximum wind speed in the boundary layer is comparable with, or even marginally higher than that above. A new feature of one of the solutions described is the existence of spatial oscillations in vertical velocity at the top of the boundary layer, inside the radius of maximum tangential wind speed. These oscillations may be interpreted as frictionally damped inertial waves. They are accompanied by annular regions in which the tangential flow alternates between supergradient and subgradient. The existence of boundary-layer induced oscillations in vertical velocity in reality would have implications for the organization of convection in the core region of a hurricane. It is shown that an approximation to determine the radial flow in the boundary layer suggested by Willoughby overestimates the vertical motion at the top of the boundary layer by a factor of about two, but the analysis leads us to question the utility of the approximation.

We investigate also the thermodynamic structure of the boundary layer and the radial distribution of surface fluxes for vortices with the same maximum tangential wind speed above the boundary layer and the same radius of maximum wind (RMW), but having different widths. It is found that the equivalent potential temperature (θ_e) in the boundary layer continues to increase with decreasing radius inside the RMW. Moreover, the negative radial gradient of θ_e in the inner core region, which is related to that of virtual temperature above the boundary layer in the eyewall region, is relatively insensitive to the vortex width, but the maximum values of θ_e increase with the width. The strength and radial distribution of the latent heat flux is insensitive to the vortex width in the inner core region, but varies markedly with width in the outer part of the vortex. Realistic radial distribution of relative humidity are obtained only when shallow convection is represented in the model. The inclusion of dissipative heating in the thermodynamic equation leads to an increase in θ_e on the order of 1.5°K in the inner core region of the vortex and to a reduction in the boundary layer relative humidity of 5 %.

1. INTRODUCTION

The frictionally-induced convergence in the boundary layer of a mature hurricane has long been appreciated to be an important feature of hurricane dynamics as this flow must eventually turn upwards to fuel the eyewall clouds with moisture laden air. What is, perhaps, less well appreciated is that, despite some frictional loss to the surface, the absolute angular momentum in the boundary layer can exceed the value immediately above the boundary layer on account of radial advection (e.g. Anthes, 1974; Shapiro, 1983; Kepert and Wang, 2001, Nguyen *et al.*, 2001). Whether or not this occurs, *the maximum wind speed*

* Meteorological Institute, University of Munich, Theresienstr. 37, 80333 Munich, Germany. Email: roger@meteo.physik.uni-muenchen.de

in the boundary layer can exceed that above the boundary layer. This feature is unusual in boundary layers, in general, and appears to be a special feature of the termination boundary layer of intense vortices. A consequence for hurricanes (and for tornadoes[†], waterspouts and dust devils) is that the maximum winds occur close to the surface. These strong low-level winds contribute to enhanced surface fluxes, drive large ocean wave fields and can do maximum damage at landfall. A further consequence is that wind *reduction* factors used to relate flight level winds observed by reconnaissance aircraft to near surface winds may be appreciably in error at inner radii (Kepert, 2001).

The central importance of the boundary layer on hurricane dynamics is highlighted in a series of papers by Emanuel (see Emanuel, 1991 and refs.; Emanuel *et al.*, 1994; Emanuel, 1995a), because of its controlling influence on the radial distribution of tropospheric heating by deep moist convection. Supported by observational studies of convecting atmospheres, Emanuel (1991) argues that the principal effect of deep convection is to bring the free troposphere to a state in which absolute angular momentum surfaces approximately coincide with reversible moist adiabats that have a saturation equivalent potential temperature equal to the reversible equivalent potential temperature, θ_e , at the top of the subcloud layer (i.e. the boundary layer). To the extent that this assumption is valid, the virtual temperature, and hence the radial density gradient at any pressure level in the troposphere is determined by the radial distribution of θ_e in the subcloud layer. In essence, convection is regarded as a type of mixing process that brings the atmosphere to a thermodynamic state that is closely related to conditions in the subcloud layer (see Emanuel *et al.*, 1994). While the accuracy of this picture is still a matter of controversy (see Stevens *et al.*, 1997; Emanuel *et al.*, 1997), the ideas are useful for gaining qualitative understanding.

As a tropical cyclone matures, the deep clouds surrounding the eye appear to be a result of slantwise moist ascent associated with frictional convergence in the boundary layer, rather than buoyant convection in the usual sense (see e.g. Willoughby, 1995 and refs; Zhu *et al.*, 2001): typically the eye is warmer than the surrounding clouds. In these clouds, the tropospheric temperature distribution along absolute angular momentum surfaces may correspond more closely to a pseudo-adiabat rather than a reversible adiabat. Nevertheless, Emanuel's arguments are qualitatively the same and reduce the problem of understanding the details of the clouds to understanding the processes that determine the distribution of boundary-layer θ_e . There are three processes involved: the surface flux of moist entropy, which is a strongly increasing function of surface wind speed; the downward flux of air with low entropy through the top of the subcloud layer associated with clear air subsidence and precipitation-cooled downdraughts; and the horizontal advection of entropy (Raymond, 1995, 1997; Emanuel, 1995a). These processes, except precipitation-cooled downdraughts, are contained in the model to be described here.

There have been several attempts to study the boundary layer of a hurricane in isolation by prescribing the wind field at the top of the layer. Smith (1968) used a momentum integral method to calculate the induced vertical velocity at the top of the boundary layer of an axisymmetric vortex on the assumption that the Ekman solution is valid at large radii where the local Rossby number is small compared with unity. The calculations were refined in papers by Leslie and Smith (1970) and Bode and Smith (1975). In the latter paper it was shown how the prescription of a generally unknown eddy diffusivity could be circumvented by including a knowledge of the surface stress and surface roughness as functions of wind speed. Shapiro (1983) studied the asymmetric boundary layer under a translating hurricane and found that the maximum convergence lies in the forward right quadrant in the northern hemisphere. One series of papers (Eliassen, 1971; Eliassen and Lystad, 1977; and Montgomery *et al.*, 2001) has considered the effects of the boundary layer on vortex

[†] Intense low-level winds were found in numerical simulations of tornado-like vortices by Rotunno (1979)

spin-down for particular initial distributions of azimuthal wind with radius. Anthes and Chang (1978) investigated the boundary layer structure of a mature hurricane in a time-dependent, axisymmetric numerical model with 9-levels, six of which were in about the lowest kilometre, but the radial resolution of 60 km was relatively coarse. Recently, Kepert and Wang (2001) carried out high resolution calculations of boundary layer structure in a dry model for both stationary and translating vortices and calculated the vertical structure of the boundary layer flow.

Many of the early hurricane models and even some more recent idealized studies assume a simple slab representation of the boundary layer. In particular, Emanuel (1995b) used such a representation in theory for the maximum potential intensity of a tropical cyclone in which vertical advection was omitted. In another study, Willoughby (1995) suggested a balanced formulation that provides a diagnostic formula for the boundary-layer inflow, but he did not investigate the accuracy of the approximation. We examine here the validity of both these assumptions using a steady, axisymmetric slab model for the boundary layer. However, the main motivation for the paper is (i) to investigate the development of high and possibly supergradient wind speeds in such a simple model for various vortex profiles, and (ii) the effects of vortex size on the radial variation of thermodynamic variables in the boundary layer, especially on the θ_e distribution.

The development of supergradient winds in the boundary layer of a hurricane means that the maximum tangential wind speed occurs in that layer rather than above it. Even if the tangential wind is not supergradient in the boundary layer, the maximum total wind speed may still exceed that above the layer. Reasons for the development of supergradient winds were suggested by Anthes (1974, p506), but he did not investigate their development in detail. Shapiro (1983) found a region of supergradient winds in the inner core of an axisymmetric vortex boundary layer, within the radius of maximum tangential wind speed above the layer, but the main focus of his study was the steady asymmetric boundary layer beneath a translating hurricane. The recent high-resolution numerical solutions of the tropical-cyclone boundary layer by Kepert and Wang (2001) found a strong radial jet in the core region in which the tangential wind speed was 10 - 25% supergradient. Nguyen *et al.* (2002) investigated the evolution of the boundary layer flow in an axisymmetric vortex model driven by buoyancy forces associated with moist convection and found the development of supergradient winds in the boundary layer. In this paper we seek to elucidate the processes involved in the development of supergradient winds.

Most of the existing boundary layer models including the detailed study by Kepert and Wang *op. cit.* have focussed exclusively on the dynamics and have not considered the moist thermodynamic structure of the layer. An exception is the paper by Anthes and Chang (1978), who calculated, *inter alia*, vertical profiles of the heat and moisture fluxes at various radii from the storm centre. An erudite review of the thermodynamic aspects of the hurricane boundary layer is given by Garstang (1979). Here we examine the influence of vortex size and structure on the radial distribution of key thermodynamic quantities in the boundary layer using our simple model.

The paper is organized as follows. The formulation of the model is described in section 2 and the representation of shallow convection in section 3. The initial conditions for the radial integration are discussed in section 4. The calculations and solution method are detailed in section 5 and the results are presented in section 6. A discussion of the results follows in section 7 and the conclusions are given in section 8.

2. THE BOUNDARY LAYER EQUATIONS

The boundary layer equations for a steady axisymmetric vortex in a homogeneous fluid on an f -plane are:

$$\frac{1}{r} \frac{\partial}{\partial r}(ru^2) + \frac{\partial}{\partial z}(uw) + \frac{v_{gr}^2 - v^2}{r} + f(v_{gr} - v) = \frac{\partial}{\partial z} \left(K \frac{\partial u}{\partial z} \right), \quad (1)$$

$$\frac{1}{r^2} \frac{\partial}{\partial r}(r^2 uv) + \frac{\partial}{\partial z}(vw) + fu = \frac{\partial}{\partial z} \left(K \frac{\partial v}{\partial z} \right), \quad (2)$$

$$\frac{1}{r} \frac{\partial}{\partial r}(ru\chi) + \frac{\partial}{\partial z}(w\chi) = \frac{\partial}{\partial z} \left(K \frac{\partial \chi}{\partial z} \right), \quad (3)$$

$$\frac{\partial}{\partial r}(ru) + \frac{\partial}{\partial z}(rw) = 0, \quad (4)$$

where (u, v, w) is the velocity vector in a cylindrical coordinate system (r, ϕ, z) , $v_{gr}(r)$ is the tangential wind speed at the top of the boundary layer, f is the Coriolis parameter, χ is a scalar quantity, taken here to be the dry static energy or the specific humidity, and K is an eddy diffusivity, taken here to be the same for momentum, heat and moisture. We assume that condensation does not occur in the boundary layer and check that saturation does not arise in the calculations. Taking the integral of Eqs. (1) - (4) with respect to z from $z = 0$ to the top of the boundary layer, $z = \delta$, and assuming that δ is a constant, we obtain:

$$\frac{d}{dr} \left(r \int_0^\delta u^2 dz \right) + [ruw]_{z=\delta} + \int_0^\delta (v_{gr}^2 - v^2) dz + rf \int_0^\delta (v_{gr} - v) dz = -Kr \frac{\partial u}{\partial z} \Big|_{z=0}, \quad (5)$$

$$\frac{d}{dr} \left(r^2 \int_0^\delta uv dz \right) + [r^2 vw]_{z=\delta} + fr^2 \int_0^\delta u dz = -Kr^2 \frac{\partial v}{\partial z} \Big|_{z=0}, \quad (6)$$

$$\frac{d}{dr} \left(r \int_0^\delta u\chi dz \right) + [rw\chi]_{z=\delta} = -Kr \frac{\partial \chi}{\partial z} \Big|_{z=0}, \quad (7)$$

$$\frac{d}{dr} \int_0^\delta rudz + [rw]_{z=\delta} = 0. \quad (8)$$

Now

$$[ruw]_{z=\delta} = ru_b w_{\delta+} + ru_{gr} w_{\delta-},$$

where u_{gr} is the radial component of flow above the boundary layer, taken here to be zero, $w_{\delta+} = \frac{1}{2}(w_\delta + |w_\delta|)$, and $w_{\delta-} = \frac{1}{2}(w_\delta - |w_\delta|)$. Note that $w_{\delta+}$ is equal to w_δ if the latter is positive and zero otherwise, while $w_{\delta-}$ is equal to w_δ if the latter is negative and zero otherwise. A bulk drag law is assumed to apply at the surface:

$$K \frac{\partial \mathbf{u}}{\partial z} \Big|_{z=0} = C_D |\mathbf{u}_b| \mathbf{u}_b,$$

where C_D is a drag coefficient and $\mathbf{u}_b = (u_b, v_b)$. Here u_b and v_b denote the values of u and v in the boundary layer, which are assumed to be independent of depth. A similar law is taken for χ :

$$K \frac{\partial \chi}{\partial z} \Big|_{z=0} = C_\chi |\mathbf{u}_b| (\chi_b - \chi_s),$$

where χ_b and χ_s are the values of χ in the boundary layer and at the sea surface, respectively. In the case of temperature χ_s is the sea surface temperature and in the case of moisture it is the saturation specific humidity at this temperature. Following Shapiro (1983, p1987) we use the formula $C_D = C_{D0} + C_{D1} |\mathbf{u}_b|$, where $C_{D0} = 1.1 \times 10^{-3}$ and $C_{D1} =$

4×10^{-5} . Further, we assume here that $C_\chi = C_D$, although there is mounting evidence that they are not the same and that neither continue to increase linearly with wind speed at speeds in excess of, perhaps, 25 m s^{-1} (Emanuel, 1995b; Emanuel, 2002, personnel communication).

Carrying out the integrals in Eqs. (5) - (8) and dividing by δ gives

$$\frac{d}{dr}(ru_b^2) = -\frac{w_{\delta+}}{\delta}ru_b - (v_{gr}^2 - v_b^2) - rf(v_{gr} - v_b) - \frac{C_D}{\delta}r(u_b^2 + v_b^2)^{1/2}u_b, \quad (9)$$

$$\frac{d}{dr}(ru_brv_b) = -r\frac{w_{\delta+}}{\delta}rv_b - r\frac{w_{\delta-}}{\delta}rv_{gr} - r^2fu_b - \frac{C_D}{\delta}r^2(u_b^2 + v_b^2)^{1/2}v_b, \quad (10)$$

$$\frac{d}{dr}(ru_b\chi_b) = -\frac{w_{\delta+}}{\delta}r\chi_b - r\frac{w_{\delta-}}{\delta}\chi_{\delta+} + \frac{C_\chi}{\delta}r(u_b^2 + v_b^2)^{1/2}(\chi_s - \chi_b), \quad (11)$$

and

$$\frac{d}{dr}(ru_b) = -r\frac{w_\delta}{\delta}. \quad (12)$$

Moreover, for any dependent variable η

$$\frac{d}{dr}(ru_b\eta) = ru_b\frac{d\eta}{dr} + \eta\frac{d}{dr}(ru_b) = ru_b\frac{d\eta}{dr} - \frac{w_\delta}{\delta}r\eta,$$

where η is either u_b , v_b or χ_b . Then Eqs. (9) and (10) become

$$u_b\frac{du_b}{dr} = u_b\frac{w_{\delta-}}{\delta} - \frac{(v_{gr}^2 - v_b^2)}{r} - f(v_{gr} - v_b) - \frac{C_D}{\delta}(u_b^2 + v_b^2)^{1/2}u_b, \quad (13)$$

$$u_b\frac{dv_b}{dr} = \frac{w_{\delta-}}{\delta}(v_b - v_{gr}) - \left(\frac{v_b}{r} + f\right)u_b - \frac{C_D}{\delta}(u_b^2 + v_b^2)^{1/2}v_b. \quad (14)$$

Equation (11) becomes

$$u_b\frac{d\chi_b}{dr} = \frac{w_{\delta-}}{\delta}(\chi_b - \chi_{\delta+}) + \frac{C_\chi}{\delta}(u_b^2 + v_b^2)^{1/2}(\chi_s - \chi_b) - R_b, \quad (15)$$

where $\chi_{\delta+}$ is the value of χ just above the boundary layer. The term $-R_b$ is added to the equation when χ is the dry static energy and represents the effects of radiative cooling, respectively.

Equations (12) - (15) form a system that may be integrated radially inward from some large radius R to find u_b , v_b , χ_b and w_δ as functions of r , given values of these quantities at $r = R$. First Eq. (13) must be modified using (12) to give an expression for w_δ . Combining these two equations gives

$$w_\delta = \frac{\delta}{1 + \alpha} \left[\frac{1}{u_b} \left\{ \frac{(v_{gr}^2 - v_b^2)}{r} + f(v_{gr} - v_b) + \frac{C_D}{\delta}(u_b^2 + v_b^2)^{1/2}u_b \right\} - \frac{u_b}{r} \right], \quad (16)$$

where α is zero if the expression in square brackets is negative and unity if it is positive. Equation (12) may be written

$$\frac{du_b}{dr} = -\frac{w_\delta}{\delta} - \frac{u_b}{r}. \quad (17)$$

3. SHALLOW CONVECTION

An important feature of the convective boundary layer (CBL) over the tropical oceans in regions of large-scale subsidence is the near ubiquity of shallow convection. Such regions

include the outer region of hurricanes. Shallow convection plays an important role in the exchange of heat and moisture between the subcloud layer, the layer modelled in this paper, and the cloudy layer above. Excellent reviews of the CBL structure are given by Emanuel (1994, Chapter 13) and Betts (1997). Over much of the tropical Pacific, for example, in regions of subsidence, the subcloud layer is typically 500 m deep and is well-mixed, with relatively uniform vertical profiles of potential temperature, specific humidity and dry or moist static energy. The cloudy layer is capped by an inversion at an altitude of about 800 mb. A similar structure was found in the outer region of Hurricane Eloise (1975) by Moss and Merceret (1976), the mixed layer depth being about 650 m in this case. The clouds, known as tradewind cumuli, are widely spaced and have their roots in the subcloud layer. They generally don't precipitate, but evaporate into the dry subsiding air that penetrates the inversion, thereby moistening and cooling the subcloud layer. In turn, the compensating subsidence in the environment of clouds transports potentially warm and dry air into the subcloud layer. This drying opposes the moistening of the subcloud layer by surface fluxes, keeping its relative humidity at values around 80 %. The equilibrium state of the CBL, including its depth and that of the subcloud layer, is governed primarily by radiative cooling, subsidence, convective transports, and surface latent and sensible heat fluxes (Emanuel, *op. cit.*, Betts, *op. cit.*). Modelling the subcloud layer requires a knowledge of the cloud-base mass flux, which together with the large-scale subsidence, determines the rate at which cloud layer air enters the subcloud layer. Emanuel (1989) used a simple cloud model to determine the mass flux of shallow convection, while Zhu and Smith (2002) use the closure scheme of Arakawa (1969), in which the mass flux is assumed to be proportional to the degree of convective instability between the subcloud layer and that above. As we do not predict the thermodynamic variables represented by $\chi_{\delta+}$ above the boundary layer, we simply choose a constant value for the mass flux of shallow convection, w_{sc} , and add this to $w_{\delta-}$ in Eqs. (13) - (15) (even if $w_{\delta-} = 0$). However, w_{δ} in Eq. (17) is left unchanged as shallow convection does not cause a *net* exchange of mass between the cloud and subcloud layers. The value for w_{sc} is chosen to ensure that the thermodynamic profile at large radius is close to radiative-convective equilibrium (see section 5).

4. STARTING CONDITIONS AT LARGE RADIUS

We have experimented with a range of starting conditions at some large radius, R , from which to begin the inward integration of the equations. It turns out that the method used by Smith (1968), who assumed that the flow above the boundary layer is in approximate geostrophic balance at large radii is adequate* for this purpose. In other words, the boundary layer at large radii is essentially governed by Ekman-like dynamics.

We assume that at $r = R$, far from the axis of rotation, the flow above the boundary layer is steady and in *geostrophic* balance with tangential wind $v_{gr}(R)$. In addition we take C_D to be a constant equal to $C_{D0} + C_{D1}v_{gr}(R)^\dagger$. Then u_b and v_b satisfy the equations:

$$f(v_{gr} - v_b) = -\frac{C_D}{\delta}(u_b^2 + v_b^2)^{1/2}u_b, \quad (18)$$

$$fu_b = -\frac{C_D}{\delta}(u_b^2 + v_b^2)^{1/2}v_b. \quad (19)$$

Let $(u_b, v_b) = v_{gr}(u', v')$ and $\Lambda = f\delta/(C_D v_{gr})$. Then equations (18) and (19) become

* "adequate" in the sense that the solution is relatively insensitive to the choice of radius R from which the integration is commenced, provided that the starting value of u_b is not too small: see section 6b.

[†] It is possible to take $C_{D0} + C_{D1}|\mathbf{u}_b(R)|$ and solve the equations for u_b and v_b numerically, but the result is essentially no difference from basing C_D on v_{gr} .

$$\Lambda(1 - v') = -(u'^2 + v'^2)^{1/2} u', \quad (20)$$

and

$$\Lambda u' = -(u'^2 + v'^2)^{1/2} y. \quad (21)$$

The last two equations have the solution

$$v' = -\frac{1}{2}\Lambda^2 + \left(\frac{1}{4}\Lambda^4 + \Lambda^2\right)^{1/2}. \quad (22)$$

and

$$u' = -[(1 - v')v']^{1/2}, \quad (23)$$

whereupon u_b and v_b follow immediately on multiplication by v_{gr} . The vertical velocity at $r = R$ can be diagnosed in terms of v_{gr} and its radial derivative using the continuity equation (12).

The starting values for the temperature T_b and specific humidity q_b in the boundary layer are 25°C and 15 g kg^{-1} , respectively, giving a relative humidity of 72%. The value for q_b is the same as the mixed layer value observed by Moss and Merceret (1976, Fig 4), but T_b cannot be compared with their observations as they showed only potential temperature.

5. THE CALCULATIONS AND SOLUTION METHOD

The steady boundary layer response to a wide range of vortex profiles $v_{gr}(r)$ has been investigated. We describe here a series of calculations for the seven profiles of tangential wind speed above the boundary layer shown in Fig. 1 and comment on pertinent results from the other calculations. The formulae for these profiles are given in the appendix. All profiles have the same maximum tangential wind speed v_m ($= 40 \text{ m s}^{-1}$) and the radius at which this occurs, r_m , is 40 km for profiles 1-6 and 100 km for profile 7. However, the profiles have different widths. Profile 6 has a secondary wind maximum at a radius of 255 km. Profile 7 is perhaps more typical of a typhoon with a large eye. In all of the calculations the value of f is taken to be $5 \times 10^{-5} \text{ s}^{-1}$ and, for reasons discussed at the end of subsection 6e, the boundary layer depth is 550 m: this depth is a comparable with the observed pressure height (950 mb) cited by Betts (1997) and a little shallower than that observed in Hurricane Eloise (1975) by Moss and Merceret (1976, Fig. 3), which showed the base of the stable layer to be at about 670 m. The sea surface temperature is taken to be 28°C . We assume that the air entering the subcloud layer from above originates from a height of 800 m, where it has a temperature, $T_{\delta+} = 22.8^\circ\text{C}$ and specific humidity, $q_{\delta+} = 15 \text{ g kg}^{-1}$, respectively. The assumption that $T_{\delta+}$ and $q_{\delta+}$ do not vary with radius is certainly a limitation, but there is little basis for doing otherwise in a boundary layer model by itself. Following Betts (1997), the radiative cooling rate that determines R_b in Eq. (15) is taken to be 2.4 deg. C. per day. The value chosen for w_{sc} is 2.2 cm s^{-1} , a value chosen so that the boundary layer is close to radiative-convective equilibrium at $r = R = 500 \text{ km}$. This value corresponds with a cloud base mass flux of 7 mb per day, which is comparable with observational estimates by Yanai *et al.* (1976) for shallow cumuli detraining below 800 mb. It is also much larger than the mean subsidence rate at $r = R$ induced by friction.

With the starting values for u_b and v_b determined by Eqs. (22) and (23), Eqs. (12) - (15) are solved using a fourth-order accurate Runge-Kutta algorithm with a radial step of 1 km for $r > 100 \text{ km}$ and 50 m for $r < 100 \text{ km}$. In each case, calculations performed with twice these values gave essentially the same results, but as the computation time is very short the higher resolution was used. As the starting radius R is increased, the radial velocity becomes small and since this quantity appears in the denominator of the differential equations, these become progressively ill-conditioned for numerical integration.

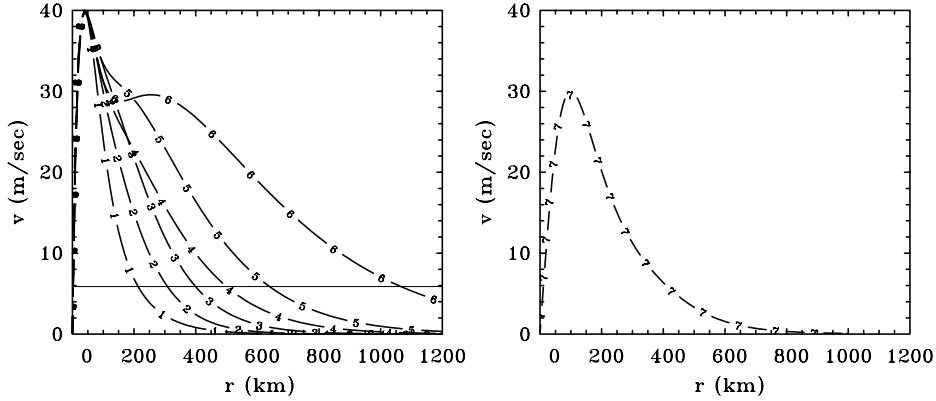


Figure 1. Radial profiles of tangential wind speed in the calculations. [Units m s^{-1}]

Therefore one has to use an increasingly smaller radial step to start the calculations, or to limit the size taken for R . The integration for the moderately broad vortex profile 4 in Fig. 1 commences at a radius $R = 500$ km. We refer to this as the control calculation. The starting value for other calculations are detailed in subsection (b).

6. RESULTS

(a) The control calculation: dynamical aspects

The behaviour in the control calculation exemplifies that in the majority of calculations. Radial profiles of selected dynamical quantities in the boundary layer and at the top of it are shown in Fig. 2 for this calculation. At large radii ($r > 350$ km), the mean vertical motion at the top of the boundary layer, \bar{w}_δ , is downward and the total wind speed $|\mathbf{v}_b| = \sqrt{u_b^2 + v_b^2}$ is less than that at the top of the boundary layer, v_{gr} . As r decreases, both u_b and v_b increase in magnitude, as does v_{gr} , the maximum value of v_b occurring just inside the radius of maximum tangential wind speed (RMW) above the boundary layer. As a result, the frictional force, $\mathbf{F} = C_d |\mathbf{v}_b| \mathbf{v}_b / \delta$ increases, and in particular its radial component, F_r , denoted by fri in the top left panel of Fig 2. The net radially-inward pressure gradient force per unit mass, $(v_{gr}^2 - v_b^2)/r + f(v_{gr} - v_b)$, denoted by pgf , increases also with decreasing r , at least for large r , but more rapidly than the frictional force. The reason is that columns of fluid partially conserve their absolute angular momentum as they converge in the boundary layer and despite some frictional loss to the surface, their rotation rate increases. The increase in v_b is assisted by the downward transfer of tangential momentum from above, represented by the term $(w_{\delta-} + w_{sc})(v_b - v_{gr})/\delta$ in Eq. (14). The main contribution is from shallow convection, the term involving w_{sc} . The downward transfer of (zero) radial momentum, represented by the term $(w_{\delta-} + w_{sc})u_b/\delta$ in Eq. (13), is denoted by wu in Fig. 2. Again the main contribution comes from shallow convection and the effect combines with friction to oppose the radial inflow. In fact the vertical advection of momentum into the boundary layer by the mean vertical motion makes a negligible contribution to the force balance in the boundary layer, supporting the approximation made by Emanuel (1995b). However the momentum transport by shallow convection, not considered by Emanuel *op. cit.*, can be seen to have a significant effect. For the typical tangential wind profile used, v_b increases faster than v_{gr} as r decreases inside a radius of about 200 km. In this region, pgf decreases faster than $wu + fri$ so that eventually the *net* radial force $pgf - wu - fri$ changes sign. This change occurs well before the RMW is reached. When $pgf - wu - fri$

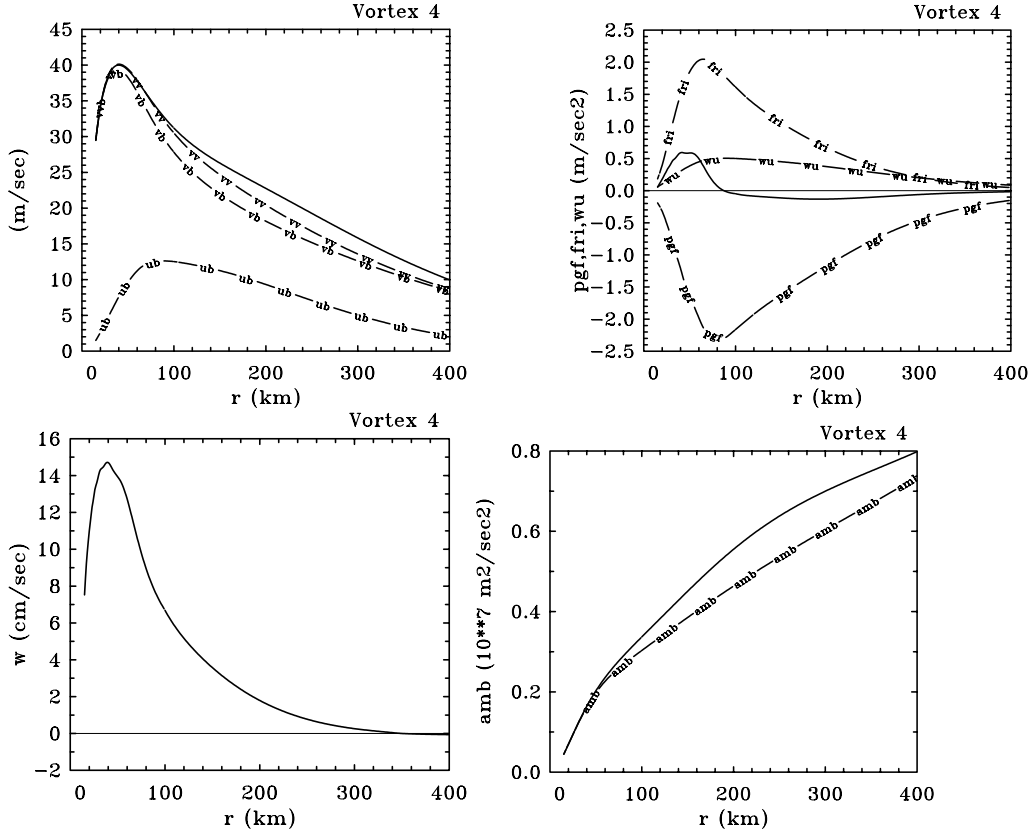


Figure 2. Radial profiles of selected dynamical quantities in the control calculation: (top left) tangential and radial components of wind speed in the boundary layer (u_b , v_b), total wind speed in the boundary layer, v_v , and tangential wind speed above the boundary layer (v_{gr} - the unmarked solid line) [Units $m s^{-1}$]; (top, right) radial pressure gradient force (pgf) and frictional force (fri) per unit mass in the boundary layer, together with the force associated with the downward flux of radial momentum through the top of the boundary layer (wu) [Units $1.0 \times 10^{-3} m s^{-2}$]; (bottom left) mean vertical velocity at the top of the boundary layer, \bar{w}_δ [Units $cm s^{-1}$]; (bottom right) absolute angular momentum above the boundary layer (solid line) and in the boundary layer (amb) [Units $1.0 \times 10^{17} m^2 s^{-2}$].

becomes positive, the radial inflow decelerates, but v_b continues to increase as columns of air continue to move inwards. Eventually, v_b asymptotes to v_{gr} and pgf tends to zero, but at no point does the tangential wind speed become supergradient. Nevertheless, as pgf tends to zero, the net outward force, primarily due to friction, becomes relatively large and the inflow decelerates very rapidly. The mean vertical velocity at the top of the boundary layer increases steadily with decreasing r and reaches a maximum very close to the RMW: thereafter it decreases rapidly.

The lower right panel of Fig. 2 shows how the absolute angular momentum in the boundary layer decreases with decreasing radius as a result of the surface frictional torque. However, the rate of decrease is less rapid than that above the boundary layer and value in the boundary layer asymptotes to the value above the layer at inner radii.

It is undoubtedly unrealistic to assume that shallow convection continues to play a role in heat, moisture and momentum transfer in the eyewall region (but perhaps not in the eye, itself). For this reason we carried out a calculation in which w_{sc} is set to zero

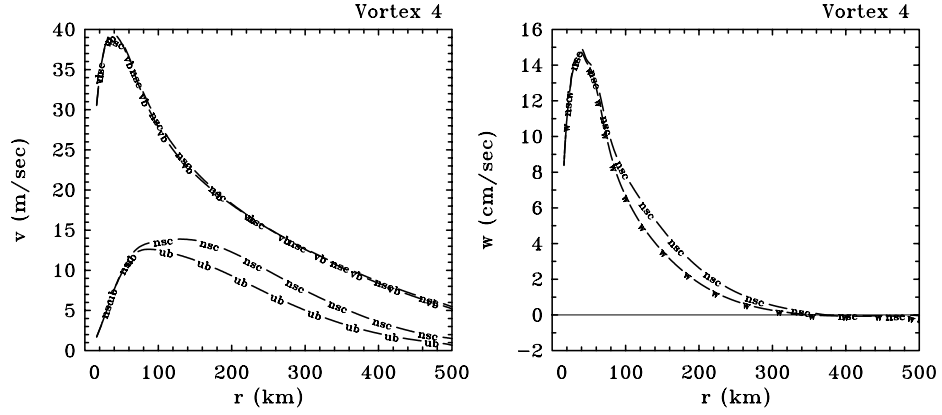


Figure 3. Radial profiles of u_b , v_b (left panel, units m s^{-1}) and \bar{w}_δ (right panel, units cm s^{-1}) in the control calculation (curves labelled "ub", "vb" and "w") and the corresponding curves for a calculation with no representation of shallow convection (curves labelled "nsc").

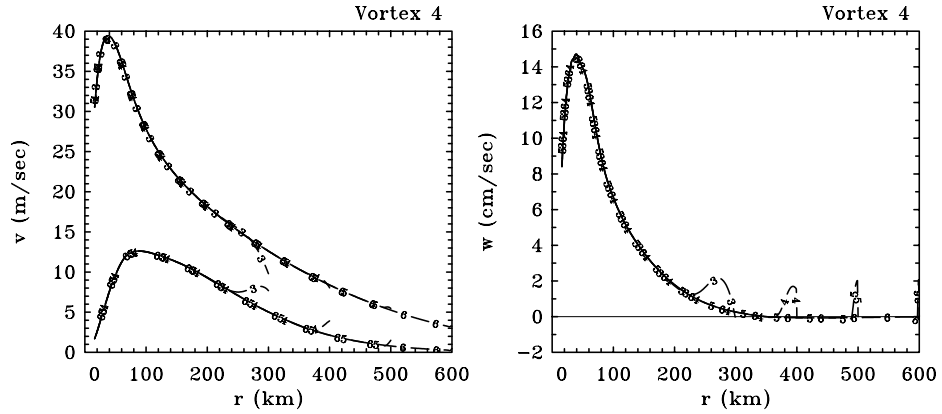


Figure 4. Radial profiles of u_b , v_b (left panel, units m s^{-1}) and \bar{w}_δ (right panel, units cm s^{-1}) in four calculations for vortex profile 4 where the starting radius R is at 300 km, 400 km, 500 km or 600 km (curves labelled "3", "4", "5" and "6", respectively).

everywhere. A comparison of the radial and tangential wind components in the boundary layer and the mean vertical velocity through the top of the layer between this calculation and the control calculation is shown in Fig. 3. The main effect of shallow convection is to bring air with zero radial momentum into the boundary layer, thereby reducing the radial wind speed in the layer and as a result the mean vertical velocity out of the layer. The lower radial wind speeds reduce the radial advection of absolute angular momentum, an effect that opposes the downward transport of this quantity so that, in this calculation at least, there is little net effect on the tangential wind speed.

(b) Sensitivity to the starting radius

Figure 4 shows radial profiles of u_b , v_b and \bar{w}_δ in four calculations where the starting radius R is at 300 km, 400 km, 500 km or 600 km. Except for a short adjustment length, which decreases in radial extent with increasing R , the curves lie on top of one another

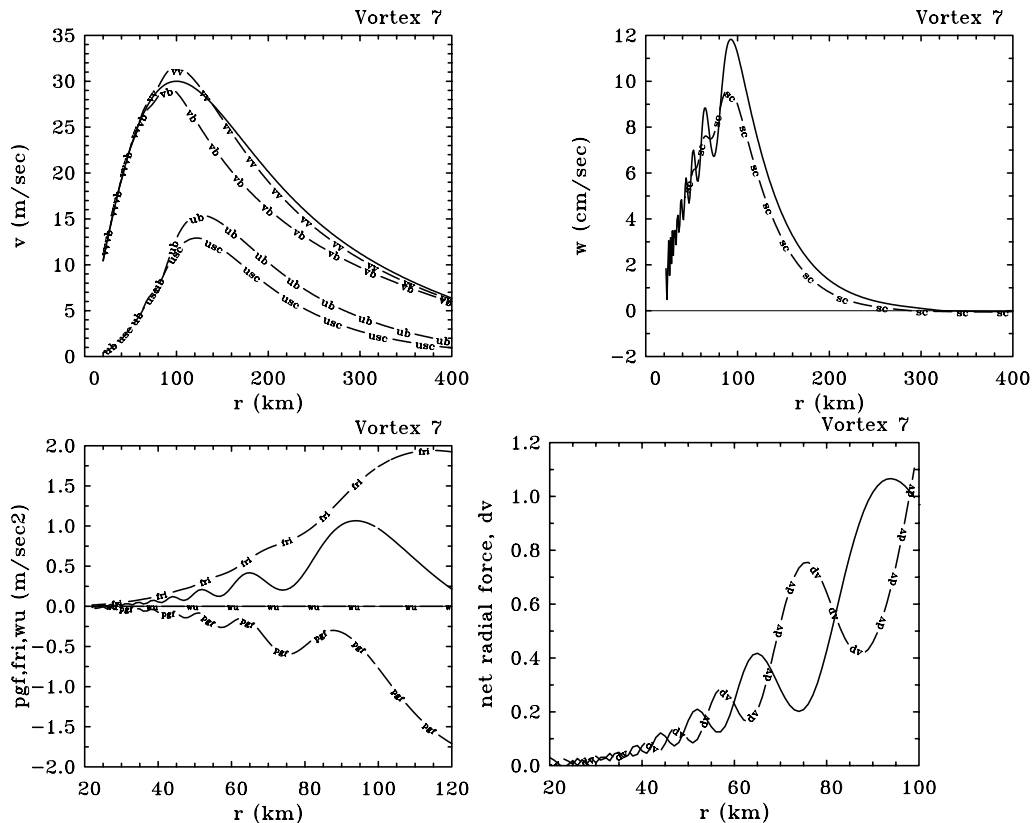


Figure 5. Legend as in Fig. 2, but the calculations relate to vortex profile 7 in Fig. 1. The curves labelled "usc", and "sc" refer to the corresponding calculation where shallow convection is included. The lower right panel compares the radial profile of net radial force with that of the velocity difference (denoted by dv) between the tangential wind component above the boundary layer and that in the layer.

indicating the relative insensitivity of the dynamics to the choice of R (subject to the caveat near the end of section 5). This insensitivity to R is not true of the thermodynamic fields as discussed in subsection (f).

(c) *Supergradient winds and inner core oscillations*

Radial profiles of total wind speed and its radial and tangential components in the boundary layer in calculations for the vortex profile 7 are shown in Fig. 5, together with the mean vertical velocity and tangential wind speed at the top of the boundary layer. Shallow convection is not taken into account. This profile has a much broader core region than in the control calculation, but the maximum wind speed is the same. The calculation shows certain important differences from those in Fig. 2, notably a series of oscillations in both boundary layer wind components and also, through continuity, in the mean vertical velocity at the top of the boundary layer. These oscillations appear to be a real feature of the model physics and not an artifact of the numerical method (halving the radial integration step produces no effective change in their structure). They are clearly associated with regular oscillations of the net radial force seen in the upper right panel of Fig. 5. In this calculation the tangential wind speed in the boundary layer becomes supergradient ($dv = v_{gr} - v_b < 0$) at a radius of about 84 km, whereupon the effective radial pressure gradient changes sign (see the lower right panel of Fig. 5). The result is a relatively large outward force on

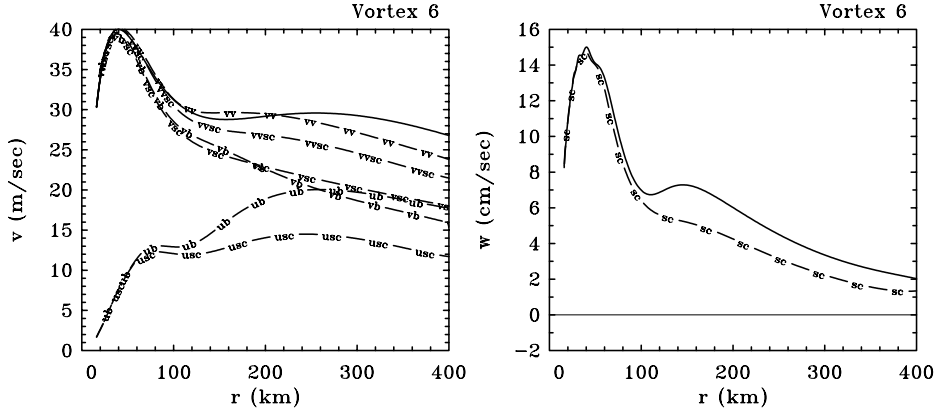


Figure 6. Legend as in the first two panels of Fig. 2, but the calculations relate to vortex profile 6 in Fig. 1, which has a secondary tangential wind speed maximum. The curves labelled "usc", "vsc", "vvsc" and "sc" refer to the corresponding calculation where shallow convection is included.

account of friction, which causes a rapid deceleration of the radial flow, thereby allowing the tangential frictional force to become subgradient once more at a radius of about 70 km. This allows the net inward radial pressure gradient to increase and the radial flow decelerates. As a result v_b increases relative to v_{gr} and again becomes supergradient. The oscillations continue as the radius decreases, but their wavelength and amplitude decline. In essence they are a kind of damped inertial wave. The inclusion of momentum transfer by shallow convection in the foregoing calculation again diminishes the inflow and thereby the amplitude of the oscillations in \overline{w}_δ (see left panels of 5). As before it has little effect on the tangential wind component, except inside the RMW, where it suppresses the development of supergradient winds.

Figure 6 shows similar calculations for vortex profile 6, which has a secondary tangential wind speed maximum above the boundary layer. Neither calculation shows a region of supergradient winds, but in the calculation without shallow convection there is a region inside the secondary wind maximum within which there is a rapid decline in the radial inflow and a local peak in the vertical velocity. The total wind speed in this calculation exceeds that in the boundary layer inside the secondary wind maximum. Small amplitude oscillations in vertical motion are apparent near the RMW in this case and again these remain present when the radial integration step is doubled. As in the previous case, vertical momentum transfer by shallow convection reduces the inflow, in this case sufficient to cause a net increase in the tangential wind speed at large radii, although the total wind speed is diminished there. Note that shallow convection has little impact on the solution near the RMW.

(d) *An approximation*

Willoughby (1995, p45) suggested an approximation for determining the radial wind speed in the boundary layer diagnostically. If the vertical advection term is neglected in Eq. (14), we obtain an expression for u_b in terms of v_b and its derivatives, i.e.,

$$u_b = -\frac{C_D v_b^2}{\delta \zeta_a}. \quad (24)$$

where $\zeta_a = dv_b/dr + v_b/r + f$ is the vertical component of absolute vorticity in the boundary layer. From this equation we may calculate the vertical velocity at the top of the boundary layer using the continuity equation (12). Figure 7 shows radial profiles of the

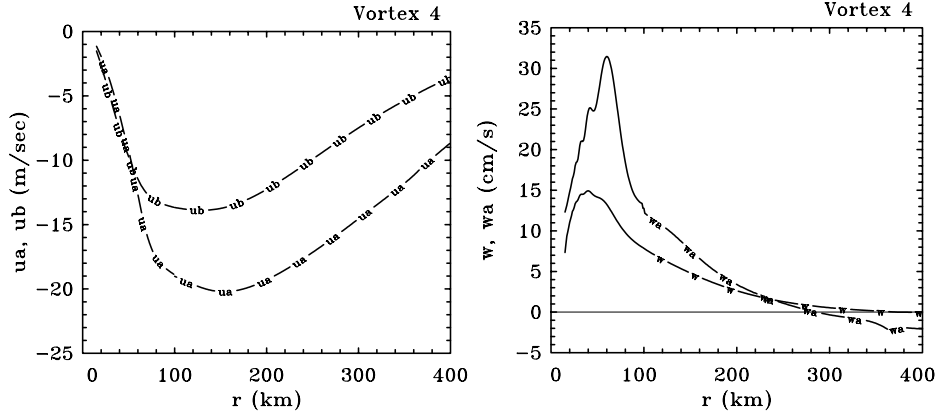


Figure 7. Left panel: radial profiles of radial wind speed in the boundary layer in the control calculation, denoted "ub" and the corresponding speed calculated using the approximate formula (24), denoted by "ua". [Units are ms^{-1}] The right panel shows the vertical velocity at the top of the boundary layer for these two inflow profiles, denoted by "w" and "wa", respectively. [Units are cm s^{-1}]

radial wind speed in the boundary layer and the vertical velocity at the top of the boundary layer in calculation 1 (defined in Table 1), together with the corresponding velocities calculated using the approximate formula (24). It can be seen that the approximate formula leads to inflow velocities and vertical velocities that are too large by factors of about two and three, respectively, compared with the unapproximated calculation. The reason can be traced to the neglect of the square of radial wind in the frictional term in Eq. (14), which, if included would decrease the denominator by a factor $\sqrt{1 - [C_D v_b / (\delta \zeta_a)]^2}$. With this factor included, the formula corresponding to (24) would be just another form of Eq. (14) at radii where the vertical flow is out of the boundary layer. Although this unapproximated form would be as easy to apply as (24) at such radii, the fact remains that both forms are really differential relations between u_b and v_b . For this reason the approximation (24) would appear to be of limited utility unless, say, ζ_a can be related to the (known) absolute vorticity at the top of the boundary layer, thereby reducing the differential relationship to an algebraic one. The boundary-layer model we describe would provide a basis for seeking such a relationship, but we do not pursue the issue here.

(e) *The control calculation: thermodynamic aspects*

The left panel of Fig. 8 shows the radial profiles of boundary layer temperature, specific humidity and saturation specific humidity, together with the saturation specific humidity at the sea surface temperature (q_{ss}), while the right panel shows the fluxes of sensible and latent heat at the surface and through the top of the boundary layer. At large radii, the wind speed is comparatively light and the boundary layer is in approximate* radiative-convective equilibrium. In particular, the air temperature just above the sea surface is only slightly lower than the sea surface temperature; the net sensible heat fluxes from the sea and through the top of the boundary layer approximately balances the radiative cooling; and the moistening of the boundary layer by the surface flux approximately balances the drying brought about by subsidence associated with shallow convection. The mass flux of shallow convection and the boundary layer depth are chosen to ensure this balance.

* The radiative-convective state is very sensitive to the choice of parameters including the mass flux of shallow convection and the boundary layer depth. We choose rounded numbers for these quantities so that the boundary layer is close to, but not exactly in equilibrium.

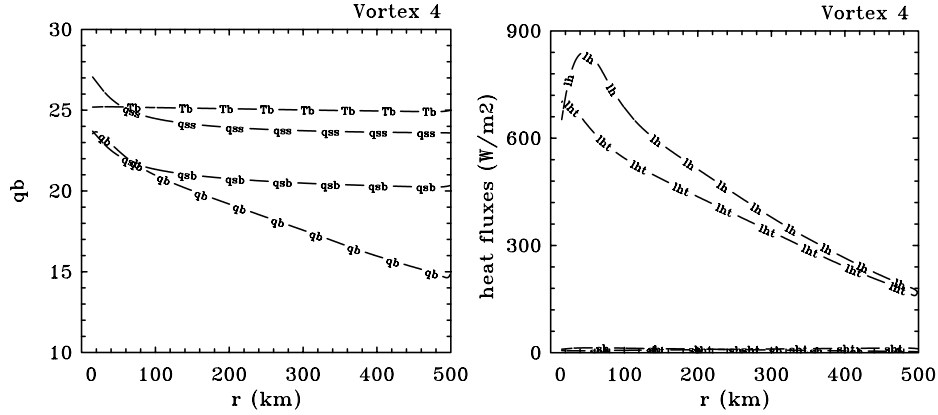


Figure 8. Radial profiles of selected thermodynamic quantities in the control calculation: (left panel) boundary layer temperature (T_b , unit deg. C), specific humidity (q_b), saturation specific humidity (q_{sb}), and the saturation specific humidity at the sea surface (q_{ss}) [Units gm kg^{-1}]; (right panel) latent heat fluxes from the sea surface (l_h) and through the top of the boundary layer (l_{ht}), and corresponding sensible heat fluxes (the two curves just above the abscissa labelled "sh" and "sht") [Units W m^{-2}].

As the r decreases and the surface wind speed increases, the surface moisture flux increases and the boundary layer progressively moistens. The increase in moisture contrast between the boundary layer and the air aloft leads to an increase in the flux of dry air through the top of the subcloud layer, which reduces the rate of moistening. This effect would be reduced in a more complete model in which the moisture content above the boundary layer is predicted. If shallow convection and radiative cooling are omitted, the rate of moistening is relatively rapid and the boundary layer saturates (i.e. $q_b = q_s$ at a relatively large radius (453 km), although, of course, then the boundary layer is not in radiative-convective equilibrium at $r = R$. In the present case, saturation occurs at a radius of about 80 km, but the air just above the sea surface does not (i.e. $q_b < q_{ss}$), which in terms of the simple model could be interpreted to mean that the boundary layer becomes topped by low cloud. A further consequence is that the surface moisture fluxes do not shut off. We have not allowed for the latent heat release in the inner core in these calculations as the degree of supersaturation is only about 1% (see Fig. 11 below). The degree of moisture disequilibrium at the sea surface is maintained by the fact that the saturation specific humidity increases as the surface pressure decreases. The right panel of Fig. 8 shows that the latent heat fluxes are much larger than the sensible heat fluxes.

(f) Moist entropy and heat fluxes

Figure 9 shows the radial profiles of reversible equivalent potential temperature in the boundary layer, θ_{eb} , and the surface flux of latent heat for vortex profiles 1 - 6. It is necessary to start these calculations at different radii in order that the boundary layer is in the same radiative-equilibrium state at $r = R$. In general there is a monotonic increase in θ_{eb} with decreasing r . The rate of increase is large when the degree of disequilibrium with the surface value is large, i.e. where the surface wind speed increases rapidly and/or the surface pressure falls rapidly. This is clearly the case for the narrower profiles at large radius, and for all profiles at inner radii.

At inner radii ($r < 60$ km), the radial gradient of θ_{eb} is similar for all six profiles although the magnitude of θ_{eb} at, say, the RMW increases as the profile broadens. Note, in particular, that θ_{eb} continues to increase inside of the RMW as the moisture fluxes remain

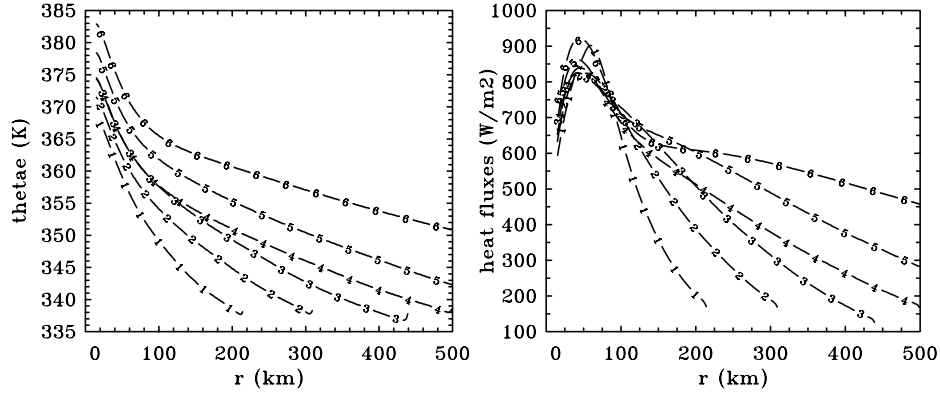


Figure 9. Radial profiles of reversible equivalent potential temperature in the boundary layer (left panel, units: deg. K), and the surface flux of latent heat (right panel, units: W m^{-2}) for vortex profiles 1 - 6 [Numbers on curves denote the profile.]

positive (left panel of Fig. 9) and the radial inflow continues to decelerate. In a recent paper, Persing and Montgomery (2002) have suggested that this continued increase may have implications for estimates of the maximum potential intensity of tropical cyclones as the current theory of Emanuel (see Bister and Emanuel, 1988 and references) assumes that the maximum value of θ_{eb} is at the RMW. We suggest that the dependence of θ_{eb} on the vortex width may be an important factor also for such estimates.

At outer radii the latent heat fluxes differ markedly between the calculations for the six profiles. In general, the fluxes are larger for the broader vortices, a reflection not only of the larger surface wind speed, but also because of the differing degree of disequilibrium between the boundary layer and the sea surface associated with a stronger inflow. This feature, as well as the fact that the starting value of R increases with the profile width, accounts for the larger values of θ_{eb} with increasing vortex size. Inside a radius of 60 km, the calculated fluxes are very similar in all calculations. The values of the fluxes are all within the range of estimated values (363 - 3600 W m^{-2}) from observations cited by Black and Holland (1995; see Tables 1 and 2 therein), which show very considerable variation themselves.

(g) The WISHE effect

In a series of papers (see Emanuel, 1991; Emanuel, 1995a,b and refs), Emanuel has highlighted the role of surface moisture flux on hurricane intensification and in particular the increase in this flux with increasing wind speed. This effect has acquired the acronym WISHE, which stands for Wind Induced Surface Heat Exchange. Emanuel argues that the sharp increase in surface moisture flux with wind speed and decreasing pressure in the inner region of a hurricane is required to elevate the boundary layer θ_{eb} to a level that can sustain the radial temperature gradient aloft in the eyewall region. The effect is demonstrated rather well by the calculations of θ_{eb} and surface moisture flux for the broad vortex profile, but with different tangential wind speed maxima (Fig. 10). For $v_m = 20 \text{ m s}^{-1}$, the moisture flux is relatively small and the increase of θ_{eb} with decreasing radius in the core is correspondingly small. However there is a marked increase in these quantities when v_m is set to 30 m s^{-1} and a further dramatic increase when it is raised to 40 m s^{-1} . As in the previous section, these calculations are carried out with different starting radii so that the starting conditions are close to the same radiative-equilibrium state.

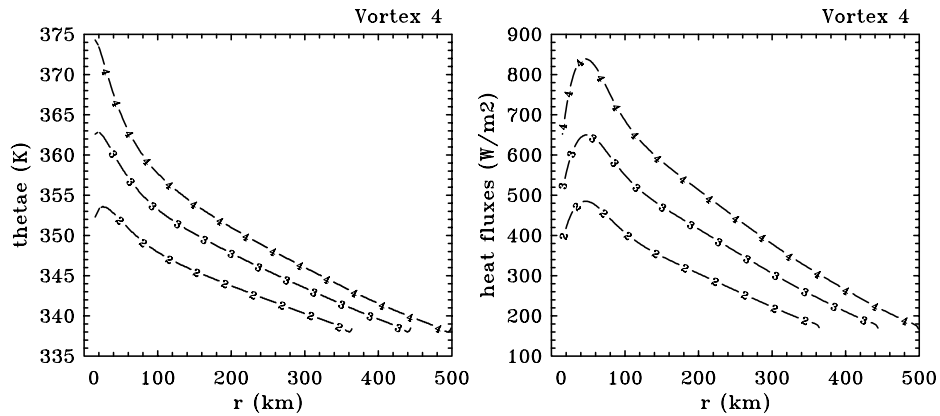


Figure 10. Radial profiles of reversible equivalent potential temperature in the boundary layer (left panel), and surface moisture flux (right panel) in the control calculation ($v_m = 40 \text{ m s}^{-1}$, curves labelled 4) and ones in which $v_m = 20 \text{ m s}^{-1}$ (curve labelled 2) and 30 m s^{-1} (curve labelled 2).

(h) Inclusion of dissipative heating

Recent estimates for the maximum potential intensity of hurricanes by Bister and Emanuel (1998) show that the inclusion of dissipative heating in the thermodynamic equation increases maximum wind speeds by about 20 %. It is of interest, therefore, to examine the effects of including dissipative heating on the boundary layer temperature, moisture and equivalent potential temperature in our model. We choose the control calculation as an example. Following Bister and Emanuel *op. cit.* (see their Eq. 6), we add a term $C_D(u_b^2 + v_b^2)^{3/2}$ to the the right-hand-side of Eq. (15) for the case in which χ_b represents the static energy. The calculations shows that dissipative heating leads to an increase in θ_e on the order of 1.5°K in the inner region and to a reduction in the relative humidity of a few per cent (right panel of Fig. 11), enough to prevent the boundary layer from saturating.

7. DISCUSSION

The model described provides a zero-order theory for the steady boundary layer of a nontranslating, axisymmetric hurricane and it is relevant to understanding the boundary-layer structure in the many hurricane models that represent the boundary layer by a single layer, including the classical early models of Ooyama, Rosenthal and Anthes (see Nguyen *et al.* (2002) for a list of references), those of Emanuel cited above, and the recent papers of Zhu *et al.* (2001), Zhu and Smith (2002), and Nguyen *et al.* (2002). Although simple models of the type described have considerable capacity to provide insight into basic processes, it is important to be aware of their limitations.

An important limitation of the model in regard to reality, even for slowly-moving storms, is the neglect of changes in boundary-layer depth. For example, the calculations by Smith (1968), Leslie and Smith (1971), and Bode and Smith (1975), and the more recent calculations by Kepert and Wang (2001) and Montgomery *et al.* (2001: see Figs. 3c and 6c) provide evidence that the boundary layer depth decreases with decreasing radius. The last two papers, indicate that the boundary layer depth is inversely proportional to the inertial stability parameter above the boundary layer (the square of the inertial stability parameter is equal to the radial gradient of absolute angular momentum squared divided by radius cubed, which is proportional to the absolute vorticity).

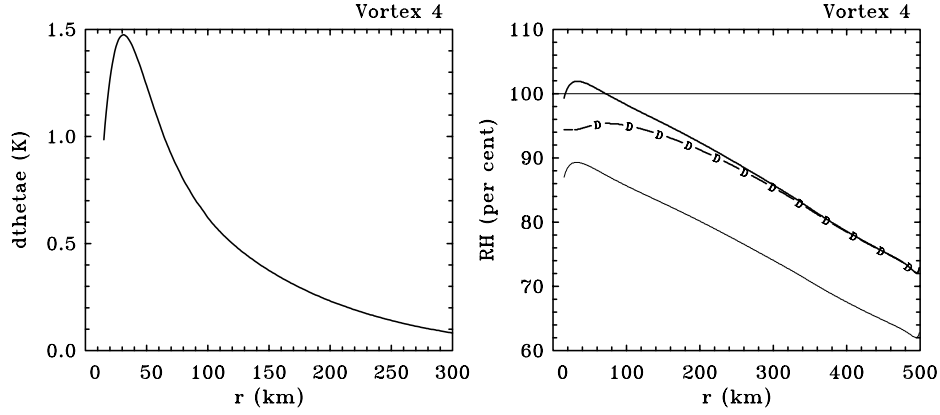


Figure 11. (left panel) Radial profile of the absolute difference in the boundary layer reversible equivalent potential temperature between the control calculation and the corresponding calculation with dissipative heating included [Units: deg. K]. The right panel compares radial profiles of boundary layer relative humidity in these two calculations (solid curve: control calculation; curve labelled "D": dissipative heating). The curve labelled "RHs" is the relative humidity of air at the sea surface temperature and the thin horizontal line indicates a relative humidity of 100 %.

While the single layer assumption should not be a limitation in estimating the vertical motion at the top of the boundary layer, which depends only on the volume flux in the boundary layer, the neglect of radial changes in boundary layer depth may be an important limitation for accurate quantitative predictions of the model (and, indeed, for any of the models that represent the boundary layer as a single layer of essentially fixed depth). In a more complete model, the boundary layer depth at large radii should be related to the surface heat fluxes, radiative cooling and the amount of mean subsidence above the tradewind inversion. In turn, these quantities should determine the mass flux of shallow convection. A further effect that has not been taken into account here is the boundary-layer cooling and drying that is associated with precipitation-cooled downdraughts from both the eyewall convection and outer rainbands. Emanuel (1995a) argues that the effects of these downdraughts should be less for a mature storm (at least in the core region), where the relative humidity of the lower troposphere has been elevated by previous convection.

The steady boundary layer equations are parabolic and require that the radial flow be unidirectional. As shown here, the solution breaks down at some radius inside the RMW, at which u_b becomes zero. Calculations using a range of profiles in addition to those investigated here show that this radius depends on the tangential wind profile above the boundary layer and is closer to the RMW when v_{gr} falls rapidly with declining radius inside the RMW. Despite the breakdown, it is reasonable to assume from a boundary-layer scaling that the calculations remain accurate to within a few boundary layer depths of this radius. Moreover, the existence of such a radius highlights the control of the boundary layer in determining the radius at which mass is expelled upwards into the eyewall clouds. Finally, it should be remembered that any complete theory of the hurricane requires the simultaneous determination of the profile of v_{gr} above the boundary layer as well as the moisture changes aloft associated with transport out of the boundary layer.

The prediction of oscillations in the vertical velocity at the top of the boundary layer in the inner core region appears to be a robust feature of the calculations (changing the radial step in the numerical integration does not change these features and they are insensitive

to the radius chosen to start the integration); indeed the existence of the oscillations can be explained physically as noted above. However, it remains to be demonstrated whether such oscillations exist if the upper vortex is allowed to adjust to the boundary layer; i.e. whether they are features of a time-dependent solution of a hurricane model, or, indeed, if the boundary layer depth is allowed to vary with radius. If the oscillations occur in nature, they would be expected to have an influence on the structure of inner-core convection. At this stage we have not succeeded in finding criteria for the existence of the oscillations in terms of the characteristics of the particular tangential wind profile.

The calculations carried out so far, including ones not reported here, do not appear to require that the tangential wind profile above the boundary layer is barotropically stable, but this might be a result of assuming a constant thickness boundary layer. For example, Kepert and Wang *op. cit.* were at pains to ensure that the profiles they chose for v_{gr} were barotropically stable, but in some calculations I investigated, there is a radius the RMW in which the radial gradient of relative vorticity above the boundary layer changes sign, this being a necessary condition for barotropic instability (Rayleigh, 1880). Recent time-dependent calculations of vortex evolution in a three-layer axisymmetric hurricane model by Nguyen *et al.* (2002) do indicate the development of regions above the boundary layer where the necessary conditions for barotropic instability are fulfilled.

8. CONCLUSIONS

Calculations based on a simple slab model for the boundary layer of a steady state, axisymmetric hurricane show that the tangential wind speed in the boundary layer approaches that above the layer in the inner core region and the maximum total wind speed in the boundary layer is comparable with, or even marginally higher than that above. One of the solutions described exhibits spatial oscillations in vertical velocity at the top of the boundary layer, inside the radius of maximum tangential wind speed. The oscillations are interpreted as frictionally damped inertial waves. The amplitude of the oscillations is reduced if the vertical transport of momentum by shallow convection is included in the calculations. Their existence in the core region of hurricanes, if confirmed, would have implications for the organization of convection. The oscillations have a maximum radial scale of about 30 km, which might be resolvable by contemporary hurricane models. Their amplitude is reduced if the vertical transport of momentum by shallow convection is included in the calculations.

The calculations indicate that an approximation to determine the radial flow in the boundary layer suggested by Willoughby overestimates the vertical motion at the top of the boundary layer by a factor of about two compared with the unapproximated theory, but our calculations lead us to question the utility of the approximation. However, they confirm the accuracy of neglecting the vertical advection terms in calculating the momentum budget, an approximation made, for example, by Emanuel in a theory for the maximum potential intensity of hurricanes.

An investigation of the thermodynamic structure of the boundary layer and the distribution of surface fluxes as a function of radius for vortices of different widths showed, *inter alia*, that the equivalent potential temperature (θ_e) in the boundary layer continues to increase with decreasing radius inside the RMW and the maximum values of θ_e increases with the vortex width. In contrast, the negative radial gradient of θ_e in the inner core region, which is related to that of virtual temperature above the boundary layer in the eye-wall region, is relatively insensitive to the vortex size for wide range of vortex profiles. The strength and radial distribution of the latent heat flux is insensitive to the vortex width in the inner core region, but varies markedly with width in the outer part of the vortex.

The inclusion of dissipative heating in the thermodynamic equation leads to an increase in the equivalent potential temperature on the order of 1.5°K in the inner core region of the vortex and to a reduction in the boundary layer relative humidity of about 5 %.

ACKNOWLEDGEMENTS

I am grateful to Kerry Emanuel, Jeff Kepert, Michael Montgomery and Hongyan Zhu for their many thought-provoking comments on earlier drafts of the manuscript. This work was supported by the US Office of Naval Research through Grant No. N00014-95-1-0394.

REFERENCES

- | | | |
|---|-------|--|
| Anthes, R. A. | 1974 | The dynamics and energetics of mature tropical cyclones. <i>Rev. Geophys. Space Phys.</i> , 12 , 495-522 |
| Anthes, R. A. and S. W. Chang | 1978 | Response of the hurricane boundary layer to changes of sea surface temperature in a numerical model. <i>J. Atmos. Sci.</i> , 35 , 1240-1255 |
| Betts, A. K. | 1997 | Trade cumulus: Observations and modelling. In <i>The physics and parameterization of moist atmospheric convection</i> (Ed. R. K. Smith), Kluwer, Dordrecht, pp99-126 |
| Bister, M., and K. A. Emanuel | 1998 | Dissipative heating and hurricane intensity. <i>Meteor. Atmos. Phys.</i> , 65 , 233-240 |
| Black, P. G., and G. J. Holland | 1995 | The boundary layer of tropical cyclone Kerry (1979). <i>Mon. Wea. Rev.</i> , 123 , 2007-2028 |
| Bode, L., and R. K. Smith | 1975 | A parameterization of the boundary layer of a tropical cyclone. <i>Bound. Layer Met.</i> , 8 , 3-19 |
| Eliassen, A. | 1971 | On the Ekman layer in a circular vortex. <i>J. Meteor. Soc. Japan</i> , 49 , (special issue), 784-789 |
| Eliassen, A. and M. Lystadt | 1977 | The Ekman layer of a circular vortex: A numerical and theoretical study. <i>Geophysica Norvegica</i> , 31 , 1-16 |
| Emanuel, K. A. | 1991 | The theory of hurricanes. <i>Ann. Rev. Fluid Mech.</i> , 23 , 179-196 |
| Emanuel, K. A. | 1995a | The behaviour of a simple hurricane model using a convective scheme based on subcloud-layer entropy equilibrium. <i>J. Atmos. Sci.</i> , 52 , 3960-3968 |
| Emanuel, K. A. | 1995b | Sensitivity of tropical cyclones to surface exchange coefficients and a revised steady state model incorporating eye dynamics. <i>J. Atmos. Sci.</i> , 52 , 3969-3976 |
| Emanuel, K. A., J. D. Neelin and C. S. Bretherton | 1994 | On large-scale circulations of convecting atmospheres. <i>Quart. J. Roy. Meteor. Soc.</i> , 120 , 1111-1143 |
| Emanuel, K. A., J. D. Neelin and C. S. Bretherton | 1997 | Reply to comments on "On large-scale circulations of convecting atmospheres". <i>Quart. J. Roy. Meteor. Soc.</i> , 123 , 1779-1782 |
| Garstang, M. | 1979 | The tropical atmospheric boundary layer: role in the formation and maintenance of hurricanes. <i>Aust. Meteor. Mag.</i> , 27 , 229-248 |
| Kepert, J. D., | 2001 | The dynamics of boundary layer jets within the tropical cyclone core. Part I: Linear Theory. <i>J. Atmos. Sci.</i> , 58 , 2469-2484 |
| Kepert, J. D., and Y. Wang | 2001 | The dynamics of boundary layer jets within the tropical cyclone core. Part II: Nonlinear enhancement. <i>J. Atmos. Sci.</i> , 58 , 2485-2501 |
| Leslie, L. M., and R. K. Smith | 1970 | The surface boundary layer of a hurricane - Part II. <i>Tellus</i> , 22 , 288-297 |

- | | | |
|--|------|--|
| Montgomery, M. T., H. D. Snell, and Z. Yang | 2001 | Axisymmetric spindown dynamics of hurricane-like vortices. <i>J. Atmos. Sci.</i> , 58 , 421-435 |
| Moss, M. S., and F. J. Merceret | 1976 | A note on several low-layer features of Hurricane Eloise (1975). <i>Mon. Wea. Rev.</i> , 104 , 967-971 |
| Nguyen, C. M., R. K. Smith, H. Zhu, and W. Ulrich | 2002 | A minimal axisymmetric hurricane model. <i>Quart. J. Roy. Meteor. Soc.</i> , 128 , In press |
| Persing, J and M. T. Montgomery | 2002 | Hurricane superintensity. Submitted to <i>J. Atmos. Sci.</i> , 59 , |
| Rayleigh, Lord | 1880 | On the stability, or instability, of certain fluid motions. <i>Proc. London Math. Soc.</i> , 11 57-70 |
| Raymond, D. J. | 1995 | Regulation of moist convection over the West Pacific warm pool. <i>J. Atmos. Sci.</i> , 52 , 3945-3959 |
| Raymond, D. J. | 1997 | Boundary layer quasi-equilibrium (BLQ). In <i>The physics and parameterization of moist atmospheric convection</i> (Ed. R. K. Smith), Kluwer, Dordrecht, 387-397 |
| Rosenthal, S. L. | 1962 | A theoretical analysis of the field motion in the hurricane boundary layer. <i>National Hurricane Research Project Report No 56</i> , US Dept of Commerce, 12pp |
| Rotunno, R. | 1979 | A study in tornado-like vortex dynamics. <i>J. Atmos. Sci.</i> , 36 , 140-155 |
| Shapiro, L. J. | 1983 | The asymmetric boundary layer under a translating hurricane. <i>J. Atmos. Sci.</i> , 40 , 1984-1998 |
| Smith, R. K. | 1968 | The surface boundary layer of a hurricane. <i>Tellus</i> , 20 , 473-483 |
| Stevens, B., D. A. Randall, X. Lin, and M. T. Montgomery | 1997 | Comments on "On large-scale circulations of convecting atmospheres" by Emanuel <i>et al.</i> <i>Quart. J. Roy. Meteor. Soc.</i> , 123 , 1771-1778 |
| Willoughby, H. E. | 1995 | Mature structure and motion. Chapter 2 of <i>A global view of tropical cyclones</i> . (Ed. R. L. Elsberry), World Meteorological Organization, Geneva, pp21-62 |
| Yanai, M., J.-H. Chu, T. E. Stark, and T. Nitta | 1976 | Response of deep and shallow tropical maritime cumuli to large-scale processes. <i>J. Atmos. Sci.</i> , 33 , 976-991 |
| Zhu, H., R. K. Smith and W. Ulrich | 2001 | A minimal three-dimensional tropical-cyclone model. <i>J. Atmos. Sci.</i> , 58 , 1924-1944 |
| Zhu, H., and R. K. Smith | 2002 | The importance of three physical processes in a minimal three-dimensional tropical cyclone model. <i>J. Atmos. Sci.</i> , 59 , 1825-1840 |

APPENDIX

The vortex profiles 1 to 6 in Fig. 1 have the form

$$v_{gr}(r) = v_1 s \exp(\alpha_1 s) + v_2 s \exp(\alpha_2 s), \quad (\text{A.1})$$

where $s = r/r_m$ and r_m , v_1 , v_2 , α_1 and α_2 are constants chosen to make $v_{gr} = v_m = 40 \text{ ms}^{-1}$ at $r = r_m = 40 \text{ km}$. With $\mu = v_1/v_m$ and α_2 specified, the values of v_1 and α_1 are given by the formulae: $\alpha_1 = (1 - \mu\alpha_2 \exp(-\alpha_2))/(1 - \mu \exp(-\alpha_2))$, and $v_1 = v_m \exp(\alpha_1)(1 - \mu \exp(\alpha_2))$. Profiles 1-6 correspond with the following pairs of values for μ and α_2 : (0.3, 0.5), (0.9, 0.5), (0.8, 0.4), (0.5, 0.3), (0.5, 0.25), (0.3, 0.15).

Profile 7 in Fig. 1 is given by the formula:

$$v_{gr}(s) = \frac{av_ms(1 + bs^4)}{(1 + cs^2 + ds^6)^2}, \quad (\text{A.2})$$

where again $s = r/r_m$, and a, b, c and d constants: $a = 1.7880$, $b = 4.74736 \times 10^{-3}$, $c = 0.339806$, and $d = 5.37727 \times 10^{-4}$. We choose $v_m = 40 \text{ ms}^{-1}$, and $r_m = 100 \text{ km}$.

Keywords hurricanes tropical cyclones typhoons boundary layers